

N. Babitha¹, S. Rosy Christy², Geetha Palani³, M. Gurumoorthy⁴, Karthik Kannan⁵,
V. Chithambaram^{6*}

Enhanced photocatalytic and Antibacterial Activity of Copper oxide Nanoparticles Synthesized by Facile Combustion methods from Mussaendafrondosa Plant Extract

¹Department of Chemistry, PERI Arts and Science College, Mannivakkam, Chennai, Tamil Nadu - 600048, India

²Department of Chemistry, Bharath Institute of Higher Education and Research, Selaiyur, Chennai, Tamil Nadu 600126

³Saveetha School of Engineering, SIMTS, Chennai - 602105, India

⁴Department of Physics, Faculty of Science and Technology, J.N.N. Institute of Engineering, Chennai - 601102, India

⁵School of Advanced Materials Science and Engineering, Kumoh National Institute of Technology (KIT), 61 Daehak-ro, Gum-si, Gyeongsanbuk-do, 39177, Republic of Korea

^{6*}Department of Physics, PERI Institute of Technology, Mannivakkam, Tamil Nadu - 600048, India
researchh.group@gmail.com

Microwave heating (MHM) and mutated sol-gel (SGM) mechanisms were used to effectively create CuO samples with two dissimilar morphologies, such as nanoparticles (CuO-NPs) and nanorods (CuO-NRs), using Mussaendafrondosalinn plant extract as the bio-reducing operator. X-ray powder diffraction (XRD), scanning electron microscopy (SEM), and energy-dispersive X-ray (EDX) investigations were used to analyze the sample's structure, pureness, and morphological characteristics. UV-Visible diffuse reflectance (DRS) and photoluminescence (PL) spectroscopy methodologies were used to analyze optical properties and calculate band gap energy. The band gap of the samples was measured using the Kubelka-Munk mechanism, and it was found to be 2.74eV and 2.33eV for CuO-NPs and CuO-NRs, correspondingly. CuO-NPs and CuO-NRs were investigated for antibacterial activity versus each Gram-positive and Gram-negative microorganisms using a modified disc diffusion method. When correlated to the sample CuO nanorods, the antibacterial study confirms that the sample CuO nanoparticles are high-grade antibacterial agents. Using solar lighting, the photocatalytic activity of CuO nano reactants (CuO-NPs and CuO-NRs) for the degradation of methylene blue (MB) dye was investigated, and the findings revealed that CuO-NPs with tinier particle sizes degraded MB more than CuONRs.

Keywords: CuO, Nanoparticles; Mussaendafrondosalinn; Antibacterial Activity; Optical Properties; Photo-Catalytic Applications.

Received 22 February 2022; Accepted 09 August 2022.

I. Introduction

Various fields like food industry, chemical industry, healthcare and electronics are embracing nanotechnology due to their many unique and desirable properties that fulfill the end users needs. When compare with all the fields, the biomedical area is greatly influenced by the nanotechnology advancement. CuO nanoparticles exhibit better biological features, especially good antibacterial

function over a broad area of pathogens and drug-resistant bacteria. CuO nanoparticles have shown their potential in pharmacological activity, specifically in anti-tumor therapy. After being recognized as antimicrobial materials by the US Environmental Protection Agency (EPA), nanoparticles of copper and its oxides have received much attention to be used in biomedical devices to prevent bacterial infection. These nanosystems are also thought to be effective possibilities in the advancement of sophisticated equipment for pathogen identification and

infection treatment [1-2].

Metal oxide nanoparticles, including copper oxide (CuO), have created attraction due to their antibacterial and biocide activities, and they could be employed in a variety of biomedical uses [3]. Copper oxide is a semiconductor metal having distinctive optical, electrical, and magnetic properties that have been employed in the construction of supercapacitors, near-infrared filters, magnetic storage media, sensors, catalysis, and semiconductors, among other uses [4-5]. CuO-NPs exhibit broad range of microbicidal activity against both bacteria. Even while CuO nanoparticles (CuO NPs) have exhibited their utility in biomedical activities, their potential for toxicity is a significant drawback for their usage in medical science [6]. The highly ionic CuO nanoparticles effectively target a wide range of bacterial pathogens associated with nosocomial infections. However, a significantly high dose of CuO-NPs is required to generate an antimicrobial effect.

CuO nanoparticles have the potential to be toxic to mammalian cells, as well as vertebrates and invertebrates. The primary toxicity mechanism is based on an enhancement in resistive oxygen species generation [6]. As a result, these nanoparticles cause oxidative discomfort in human pulmonary epithelial cells, increase toxicity, and damage DNA and mitochondria [7-8]. In the present study, we have been focused on synthesizing and characterizing CuO nanoparticles from *Mussaendafrondosa* Plant Extract, and investigating catalytic activities and potential biological of these nanoparticles. Full investigation in terms of biological activities from antibacterial and antifungal towards cellular toxicity assessments were accomplished with details.

II. Experimental methods

2.1. Synthesis of CuO nanoparticles and nanorod

Mussaendafrondosa leaves were collected from local areas of Calicut district, Kerala. The 5gram of leaves were washed, boiled in 10ml de-ionized water stirred for 30 min and the excerpt was obtained. 0.241 g of copper nitrate - plant extract was placed in a microwave oven for 10mints. The powder obtained was cleaned with ethanol and dehydrated to 70°C for half an hour.

To make a well-dissolved solution, 0.241g of Copper nitrate was gently mixed to 10 ml of *Mussaendafrondosa* plant extract underneath continuous stirring for 2 hours. *Mussaendafrondosa* plant extract has performed both bio-reducing and gelling agents in this way. In a typical microwave oven, the precursor combination of Copper nitrates in *Mussaendafrondosa* plant extract was subjected to microwave energy in a 2.45GHz multi-mode cavity at 800 W for 10 minutes. The precursor combination at first boiled and disintegrated with the release of substantial concentrations of gases, resulting in solid powders [9-10]. After that, the powder was rinsed in ethanol and dried for 30 minutes in an electric oven at 70°C.

The discovered powders were assigned as CuO nanoparticles. The remaining precursor mixture sol (Copper nitrate and *Mussaendafrondosa* plant extract)

was placed on a hot plate and evaporated by heating at 100°C with continuous stirring for certain hours till a gel was produced. The gel was removed from the hot plate and smashed into powder with a mortar and pestle before being calcinated in a muffle furnace at 500°C for 2 hours at a rate of 5°C per minute. The solid powders formed were identified as copper nitrate metal oxide [11].

III. Results and Discussion

3.1. FT-IR Analysis

The FT-IR spectra of composite samples are shown in Figure 1. The sample's FT-IR transmission spectra were obtained in the region of 400-4000 cm^{-1} , which was utilized to evaluate the functional groups. The notable peak around 1629 cm^{-1} is a CuO bond characteristic peak. At 1618 cm^{-1} , the band corresponds to asymmetrical H-O-H. The faint absorption peak of 1346 cm^{-1} was attributed to hydroxyl (bending), which represented water in the sample as moisture [12]. Since nanocrystalline materials have a strong surface to volume proportions and consume dampness, the broad absorption at around 3320 cm^{-1} implies the appearance of a hydroxyl group (stretching) accumulated water. The existence of water molecules on the oxide surface may play an important function in optimizing the prepared sample's photo catalysis.

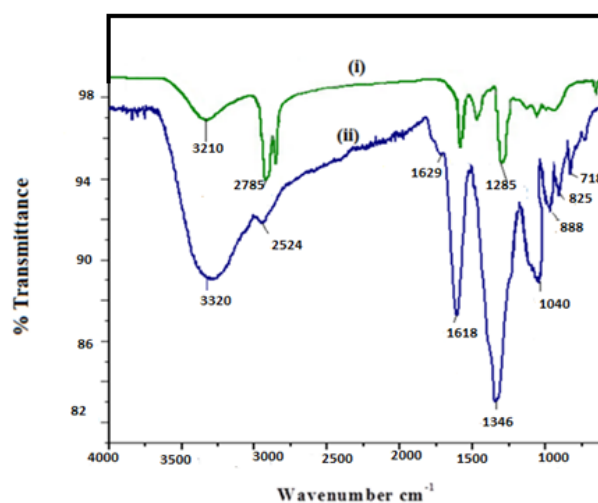


Fig. 1. FTIR spectra(i) CuONPs (ii) CuONRs.

3.2. UV-Visible spectra analysis

At ambient temperature, optical diffuse reflectance (DR) spectra of CuO nanoparticles and CuO nanorods samples were measured. The basic absorption of electron excitation from the valence band to the conduction band is often employed to calculate the optical bandgap. An important element for photo-catalytic activity is the optical absorption wavelength of the produced sample. An important element for photo-catalytic activity is the optical absorption wavelength of the produced sample. When enough electrons are stimulated from the valence band (VB) to the conduction band (CB), the photocatalytic behavior of the nano-catalyst will be productive. The energy of incident light is provided by a catalyst with bandgap energy equal to or greater than that of photocatalysts. The bandgap energy was calculated by the

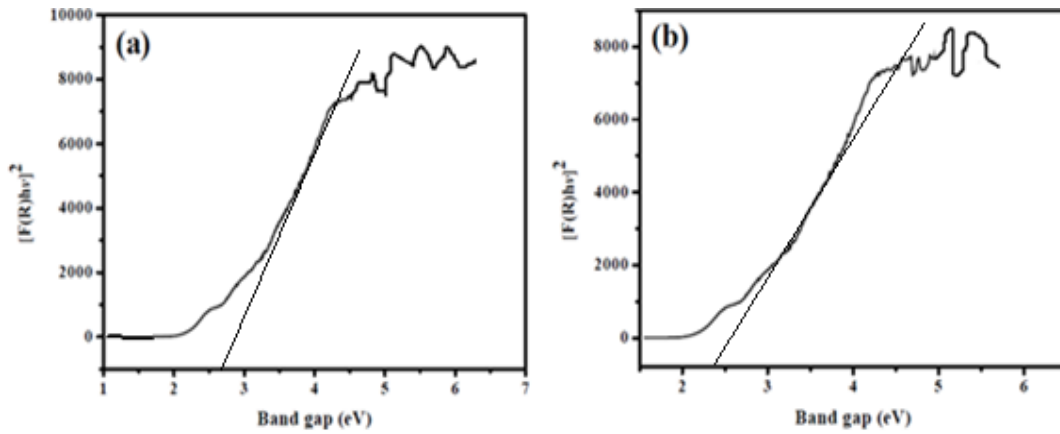


Fig. 2. UV-Vis band gap of CuO nanoparticles and CuO nanorods.

Tauc formulation, $(\alpha hv)^{1/n} = A (hv - E_g)$, in which h is Planck's constant, ν is vibration frequency, α is absorption coefficient, E_g is bandgap energy, and A is a proportionality constant and n is sample transition behavior [13].

The curve of (αhv) versus hv is shown in Figure 2. Extrapolation of linear segments in $[\alpha hv]$ against hv plots yields CuO nanoparticles and CuO nanorods samples have E_g values of 2.74 and 2.33 eV, correspondingly. The particle size and morphology of the samples are primarily responsible for the observed variation.

3.3. Powder XRD Analysis

Figure 3 shows the powder X-ray diffraction patterns of CuO nanoparticles. Both samples have exact diffraction peaks, indicating that they are crystalline. These planes are then related d -spacing values of 3.61, 2.62, 2.53, 2.24, 1.85, 1.66, 1.47, and 1.48 Å, which are ascribed to the CuO rhombohedra phase. The cubic form of CuO has been assigned to this arrangement, with lattice parameters of $a = b = c = 8.351 \text{ \AA}$. CuO is the sole peak evident because there are no other peaks. For coupled metal oxides, the particle size is estimated employing the Scherrer methodology. The strong peaks show that the crystallite size of the CuONPs sample is larger than that of CuONRs. Because of the high-temperature calcination (CCM technique, $500^\circ\text{C}/2\text{hr}$), the mean crystallite size (d) of CuONPs is 30.42 nm, which is smaller than CuONRs (39.55 nm). The crystallite size grew as the temperature raised, according to the studies. Such findings have been published (Jiang et al., 2010) [14].

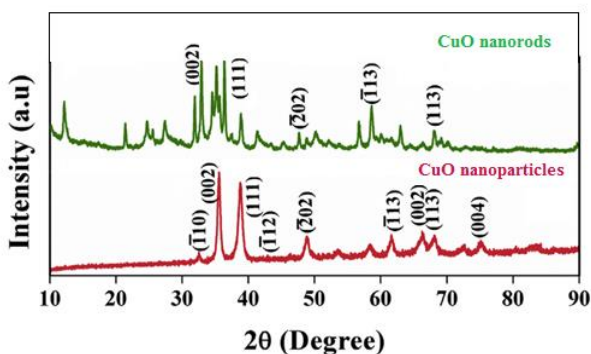


Fig. 3. Powder XRD patterns of (a) CuONPs and (b) CuONRs samples.

$$\sin^2 \theta = \frac{\lambda^2}{4} \left[\frac{3}{4} \left(\frac{h^2 + hk + k^2}{\alpha^2} \right) + \frac{l^2}{c^2} \right]$$

The formula in the equation was used to compute the lattice parameters. Where θ is the diffraction angle, λ incident wavelength ($\lambda = 1.540 \text{ \AA}$), and Miller's indices h , k , and l . The sample CuO nanoparticles have lattice parameters of $a = 5.033 \text{ \AA}$ and $c = 13.744 \text{ \AA}$, while the sample CuONRs has lattice parameters of $a = 5.022 \text{ \AA}$ and $c = 13.736 \text{ \AA}$.

Table 1.

Structural parameters, lattice constant and crystallite size (CuO-NPs and CuO-NRs) nanomaterials

Samples	Lattice parameter values (Å)			Crystallite size (L) (nm)
	(a)	(c)	c/a	
CuO-NPs	5.033	13.744	2.730	30.42
CuO-NRs	5.022	13.736	2.735	39.55

3.4. HR-SEM and energy dispersive X-RAY (EDAX) analysis

EDAX assessment was used to identify the elemental composition and phase clarity of the samples, and the spectrum is presented in figure 4 (a), (b), which reveals the elemental content of ZnO-NPs and ZnO-NSs, correspondingly. It demonstrates the presence of O and Zn elements but no additional signals, implying that the products are pure form [15]. The surface morphology of the as-prepared samples was investigated utilizing a high-resolution scanning electron microscope (HR-SEM). HR-SEM studies were used to examine the structures of the CuONPs and CuONRs samples in greater aspects. Figure 4 (a,b) and Figure 5 (a,b) show HR-SEM images of CuONPs and CuONRs samples at various magnifications. cups are asymmetrical sphere nanoparticles joined tightly by agglomeration, as evidenced by the sample. CuO has a greater electron binding energy. The particles are accumulated as a result of the heat created throughout the process, according to the HRSEM studies. XRD computations evaluate the expanded crystalline range that coherently diffracts X-rays, whereas SEM findings are focused on the variation across visible grain boundaries. As a result, the XRD methodology has a stricter requirement and produces smaller sizes.

The production of multiple micrometer-long nanorod bundles with unit rod widths of around 100 nm and a Cu/O

proportion of 1:1 are revealed by SEM/EDAX. Individual rod diameters of 40–80 nm (mean 60 nm with a normal variation of 9.74 nm) and rod lengths of 4–11 μm (mean 8 μm with a normal variation of 1.87 μm) are found in regularly produced nanorod bundles [16]. EDX investigation was used to identify the elemental composition and phase clarity of the samples, and the spectrum is given in Figure 5 (a), (b), which reveals the elemental content of CuO-NPs and CuO-NRs, separately. It reveals the appearance of O and Cu components, with no other possible signs, indicating that the compounds are

a strong element.

3.5. TEM and SAED analysis

Internal micro/nanostructure materials are analyzed using a transmission electron microscope (TEM). A high-resolution transmission electron microscope is used to image the crystal arrangement of the samples on an atomic level (HR-TEM). The spherical form of the particles generated by this process was validated by TEM images. The sample's grain sizes were also reported to be less than 40nm. The crystallite sizes of the samples estimated from

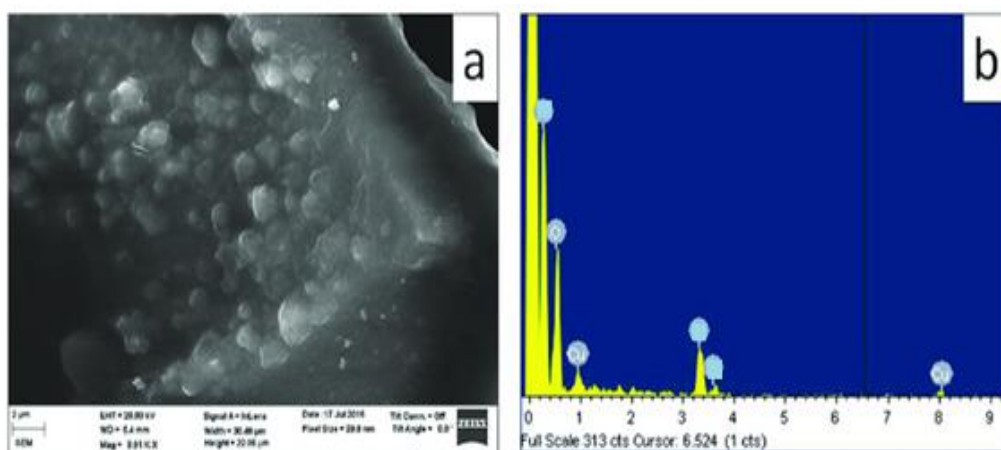


Fig. 4. (a) SEM image of CuO nanoparticles (b) EDAX spectra of CuO nanoparticles.

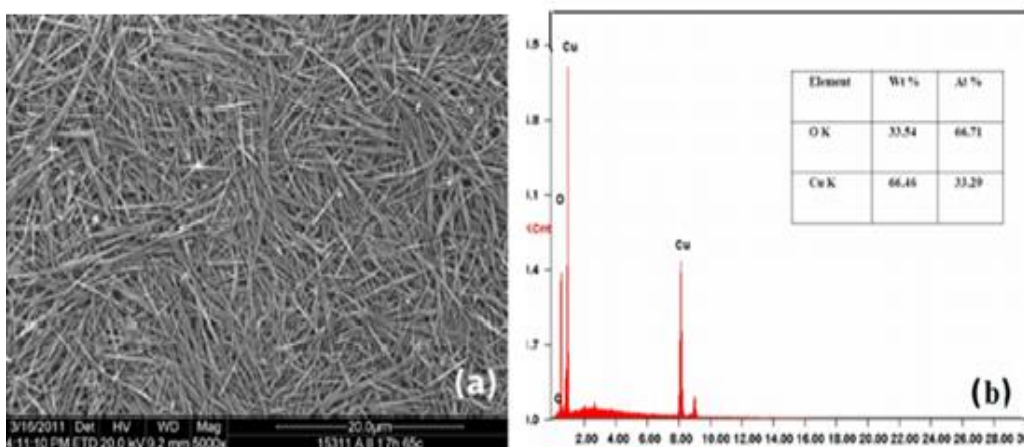


Fig. 5. (a) SEM image of CuO nanorods (b) EDAX spectrum of CuO nanorods.

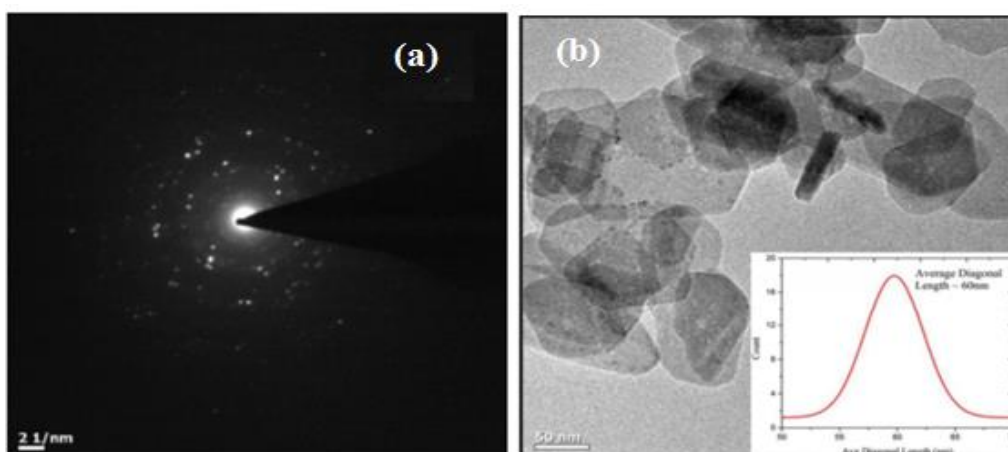


Fig. 6. (a) SAED Pattern of CuO nanoparticles (b) TEM image of the CuO nanoparticles.

powder-XRD measurements were validated by TEM micrographs. CuO nanoparticles selected area electron diffraction (SAED) pattern is shown in Figure 6a. The nanoscale rings comprising of well-crystalline elements [17] have a continuous and dispersed character. The synthesis of extremely crystalline nanoparticles is indicated by the appearance of discrete diffraction patterns.

IV. Photocatalytic Activity

The amount of deterioration of an aqueous Methylene blue (MB) solvent in the existence of a catalyst with UV light is determined by photocatalytic degradation activity. The absorption peaks of MB's UV spectra are located at 588 nm. H_2O_2 creates two hydroxyl radicals (HO^*) in the appearance of Ultraviolet irradiation, which contributes to the disintegration of MB. For the disintegration of natural waste products, the HO^* are regarded as notably vigorous oxidants.

Dye degradation occurs in a variety of mechanisms, including direct hydroxyl radical action, photo-induced electron reduction, and indirect oxidation in the existence of holes [18]. Because the photocatalytic oxidation-reduction process occurs primarily on the interface of photocatalysts, the surface parameters have a significant impact on the catalyst's performance. However, morphology can also play a role in determining the actual degradation performance. When the photo-Fenton process was started by bringing illumination and H_2O_2 to the system, there was a noticeable degradation of CV. CuONPs and CuONRs samples, on the other hand, had a higher degradation activity due to their small band gap and larger absorption wavelength range, which caused visible light to be absorbed and additional electrons and holes to be produced in photocatalytic degradation. Figure 7a shows the photo degradation of the MB dye sample. When the duration is increased, the percentage of degradation increases as well; the CuONPs performance for MB dye is 93%. When contrasted to the remaining CuONRs sample, it is higher (Table 2). In the presence of CuO nanorods, NB was successfully photo degraded under visible light irradiation. In general, photocatalytic degradation of MB is dependent on various experimental conditions such as catalyst dose, pH of the reaction medium, and MB concentration [18]. To know the best degradation conditions; the degradation was carried out at different experiments. Initially, NB was subjected to visible light radiation for 150 minutes and MB was not degraded under visible light irradiation. There was significant degradation of MB in the existence of CuO nanorod as photocatalyst.

Table 2.

Photo-catalytic degradation efficiency of CuO nanoparticles and CuO nanorods samples

Photocatalyst Sample code	PCD efficiency (%)
CuONPs	93%
CuONRs	87%

In presence of CuO nanoparticles, MB was

successfully photo degraded under visible light irradiation. In general, photocatalytic degradation of MB is dependent on various experimental conditions such as catalyst dose, pH of reaction medium, and MB concentration. To know the best degradation conditions; the degradation was carried out at different experiments [19]. Initially, MB was subjected to visible light radiation for 135 minutes and MB was not degraded below visible light irradiation. In Figure 7b the absorption peaks at 664, corresponding to MB are shown to degrade and disappear after 135 minutes.

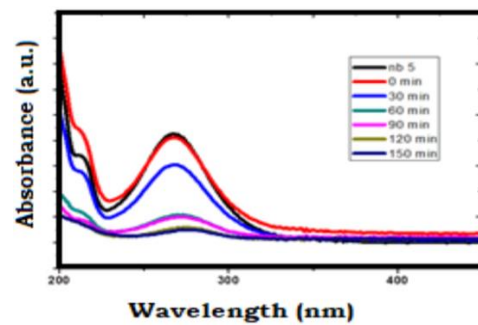


Fig. 7a. Photocatalytic degradation of MB under UV light irradiation of CuO nanorods.

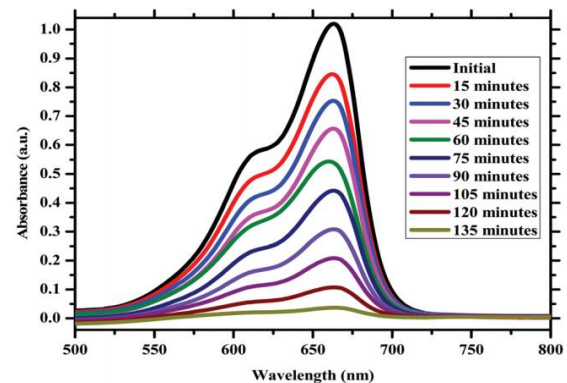


Fig. 7b. The absorption spectra for the photocatalytic degradation of MB using Cu nanoparticles.

V. Antibacterial Activity

Both gram-negative and gram-positive bacteria were used to assess the antimicrobial activity of the produced samples. The 24h bacterial cultures were scrubbed in Muller Hinton agar enhanced plates. Whatmann filter paper discs with a thickness of 3 mm were saturated with 100 μ L of a solution comprising CuO nanoparticles and nanorods and allowed to evaporate for 1 hour. To compare the antibacterial performance of the samples, reference standard discs containing ampicillin (10g/mL) were made. The discs were placed in swabbed bacterial plates and treated at 28°C for 24 hours after dehydrating. Plates were evaluated after incubation for a clean region surrounding the discs. Antibacterial activity was measured in a clean zone with a diameter of more than 2 mm. The antibacterial performance of CuO nanoparticles region of inhibition versus (a) E.coli and (b) Calibicans is shown in Figure 9.

When contrasted to the sample CuO nanorod, the antibacterial examination confirms that the sample CuO

nanoparticles are high-standard antibacterial weapons [20]. Because smaller particles require more particles to fill a bacterial colony, active oxygen species are generated, which destroy bacteria very successfully.

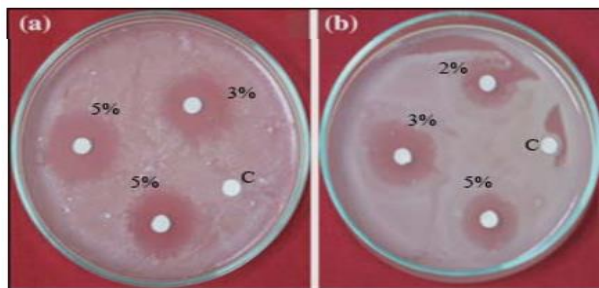


Fig. 9. Antibacterial activity of CuO nano Particles zone of inhibition against (a) E.coli (b) Calibicans.

Table 3.

Shows Bacteria and fungus organism test by CuO nanoparticles

Antibacterial activities of samples were determined as zone of inhibition (in mm)		
Samples	E.Coli	Caibicans
Ampicillin (C)	12	14
CuONPs	14	9
CuONRs	13	9

VI. Conclusions

CuO nanoparticles were synthesized by two different combustion methods namely microwave and conventional combustion methods using *Mussaendafrondosa* plant extract as the diminishing factor and were portrayed employing standard techniques. From the powder X-Ray studies, the crystallite size of the CuONPs sample is higher compared to that of CuONRs indicated by the sharp

peaks. The average crystallite size of CuONPs is 30.42 nm, which is lower than the CuONRs (39.55 nm), due to the high-temperature calcinations (CCM method, 500 °C/2hr). Band energy gap values of CuO nanoparticles and CuO nanorods samples are 2.74 eV and 2.33 eV separately. The morphologies of the CuONPs and CuONRs samples were inspected in detail using HR-SEM analyses. The crystallite sizes of the samples obtained from powder XRD spectroscopy were validated by TEM images. The role of photocatalysis in the degradation of MB was studied. When compared with the CuO nanorods sample, CuO nanoparticles showed maximum catalytic activity with higher efficiency.

The decline in absorption optimum of the MB degrading investigation revealed that CuO nanoparticles degraded by 93 percent in 135 minutes owing to a combination of parameters including crystallite size, oxygen deficiencies, and bandgap ranges. When matched to the sample CuO nanorods, the antibacterial study confirms that the sample CuO nanoparticles are top-quality antimicrobial weapons.

Babitha N. (PhD) – PERI Arts and Science College, Mannivakkam, Chennai, Tamil Nadu, India;

Rosy Christy S. (PhD) – Bharath Institute of Higher Education and Research, Selaiyur, Chennai, Tamil Nadu 600126;

Palani Geetha (PhD) – Saveetha School of Engineering, SIMTS, Chennai - 602105, India;

Gurumoorthy M. (M.Sc., (PhD)) – Faculty of Science and Technology, J.N.N. Institute of Engineering, Chennai - 601102, India;

Kannan Karthik (PhD) – School of Advanced Materials Science and Engineering, Kumoh National Institute of Technology (KIT), 61 Daehak-ro, Gum-si, Gyeongsanbuk-do, 39177, Republic of Korea;

Chithambaram V. (PhD) – PERI Institute of Technology, Mannivakkam, Tamil Nadu - 600048, India.

- [1] M.E. Grigore, E.R. Biscu, A.M. Holban, M.C. Gestal, and A.M. Grumezescu, Methods of Synthesis, Properties and Biomedical Applications of CuO Nanoparticles, Pharmaceuticals 9, 75 (2016); <https://doi.org/10.3390/ph9040075>.
- [2] S. Nations, M. Long, M. Wages, J.D. Maul, C.W. Theodorakis, G.P. Cobb Subchronic and chronic developmental effects of copper oxide (CuO) nanoparticles on *Xenopus laevis*. Chemosphere 135, 166 (2015); <https://doi.org/10.1016/j.chemosphere.2015.03.078>.
- [3] Vasantharaj S, Sathiyavimal S, Saravanan M, et al. Synthesis of ecofriendly copper oxide nanorods for fabrication over textile fabrics: characterization of antibacterial activity and dye degradation potential. J Photochem Photobiol B 191(191), 143–149 (2019); <https://doi.org/10.1016/j.jphotobiol.2018.12.026>.
- [4] Chuanpan Guo, Fang Cheng, Gaolei Liang, Shuai Zhang, Qiaojuan Jia, Linghao He, Shuxia Duan, Yingkun Fu, Zhihong Zhang, Miao Du. Copper-based polymer-metal–organic framework embedded with Ag nanoparticles: Long-acting and intelligent antibacterial activity and accelerated wound healing. Chemical Engineering Journal, 435, 134915 (2022); <https://doi.org/10.1016/j.cej.2022.134915>.
- Xiong, L. et al. Size-controlled synthesis of Cu₂O nanoparticles: size effect on antibacterial activity and application as a photocatalyst for highly efficient H₂O₂ evolution. RSC Adv. 7, 51822–51830 (2017); <https://doi.org/10.1039/C7RA10605J>.
- [5] P. Geetha, et.al., Growth, Spectroscopic, Dielectric & Electrical studies of Glycine Manganous Acetate Single Crystal, International Journal of ChemTech Research 9(07), 324-333 (2016).
- [6] Yang, Z. et al. Long-term antibacterial stable reduced graphene oxide nanocomposites loaded with cuprous oxide nanoparticles. J. Colloid Interface Sci. 533, 13–23 (2019); <https://doi.org/10.1016/j.jcis.2018.08.053>.
- [7] K Kannan, et.al., Facile fabrication of novel ceria-based nanocomposite (CYO-CSO) via co-precipitation: Electrochemical, photocatalytic and antibacterial performances, Journal of Molecular Structure, 132519 (2022); <https://doi.org/10.1016/j.molstruc.2022.132519>.

- [8] Beena, V., Ajitha, S., Rayar, S.L. et al. Enhanced Photocatalytic and Antibacterial Activities of ZnSe Nanoparticles, *J Inorg Organomet Polym* 31, 4390–4401 (2021); <https://doi.org/10.1007/s10904-021-02053-7>.
- [9] Prashansa Sharma, et.al., Green synthesis and characterization of copper nanoparticles by *Tinospora cardifolia* to produce nature-friendly copper nano-coated fabric and their antimicrobial evaluation, *Journal of Microbiological Methods*, 160, 107-116 (2019); <https://doi.org/10.1016/j.mimet.2019.03.007>.
- [10] Geetha Palani, et.al, Growth, characterization and antibacterial activity of LHCdBr single crystal, *Materials Research Innovations* 25(4), 208-214 (2021); <https://doi.org/10.1080/14328917.2020.1814028>.
- [11] D Radhika, et.al., Gd³⁺, and Y³⁺ co-doped mixed metal oxide nano hybrids for photocatalytic and antibacterial applications, *Nano Express* (2021); <https://doi.org/10.1088/2632-959X/abdd87>.
- [12] V Chithambaram et.al., A study on structural, microhardness, dielectric and antimicrobial properties of TSMnAc crystal, *Pages* 208-214, May (2020); <https://doi.org/10.1080/14328917.2020.1772448>.
- [13] Chinnaiiah, K., Maik, V., et al. Experimental and Theoretical Studies of Green Synthesized Cu₂O Nanoparticles Using Datura Metal L. *J Fluoresc* (2022); <https://doi.org/10.21203/rs.3.rs-804953/v1>.
- [14] A Rangayasami, et.al., Information and Advanced Technology Applied at Agriculture and Livestock Development, *Agro-biodiversity and Agri-ecosystem Management*, 323-339 (2021); https://doi.org/10.1007/978-981-19-0928-3_17.
- [15] Bharathi, D.S., Boopathyraja, A., Nachimuthu, S. et al. Green Synthesis, Characterization and Antibacterial Activity of SiO₂-ZnO Nanocomposite by *Dictyota bartayresiana* Extract and Its Cytotoxic Effect on HT29 Cell Line. *J Clust Sci* (2021); <https://doi.org/10.1007/s10876-021-02170-w>.
- [16] TetianaTatarchuk, et.al., Eco-friendly synthesis of cobalt-zinc ferrites using quince extract for adsorption and catalytic applications: An approach towards environmental remediation, *Chemosphere* 294, 133565 (2022); <https://doi.org/10.1016/j.chemosphere.2022.133565>.
- [17] C Pravallika, et.al, Crystal growth, spectroscopic and antimicrobial investigations on glycine-doped ZnSO₄-(NH₄)₂SO₄ single crystal, *Journal of Materials Science: Materials in Electronics* 32(10), 13917-13925 (2021); <https://doi.org/10.1007/s10854-021-05967-7>.
- [18] K. Karthik, et.al., Facile microwave-assisted green synthesis of NiO nanoparticles from *Andrographis paniculata* leaf extract and evaluation of their photocatalytic and anticancer activities, *Published online: 19 June 2022*, 70-80 (2019); <https://doi.org/10.1080/15421406.2019.1578495>.
- [19] TetianaTatarchuk, Photocatalytic degradation of dyes using rutile TiO₂ synthesized by reverse micelle and low-temperature methods: real-time monitoring of the degradation kinetics, *Journal of Molecular Liquids* 342, 117407 (2021); <https://doi.org/10.1016/j.molliq.2021.117407>.

Н. Бабіта¹, С. Р.Хрісті², Г. Палані³, М. Гурумурзі⁴, К. Каннан⁵, В. Чітамбарам^{6*}

Посилена фотокаталітична та антибактеріальна активність наночастинок оксиду міді, синтезованих методами легкого спалювання з рослинного екстракту *Mussaendafrondosa*

¹Кафедра хімії, PERIколедж наук та технологій, Манніваккам, Ченнаї, Таміл Наду - 600048, Індія

²Кафедра хімії, Технологічний інститут PERI, Манніваккам, Таміл Наду - 600048, Індія

³Школа інженерії Савіта, SIMTS, Ченнай- 602105, Індія

⁴Кафедра фізики, факультет науки і технологій, Інженерний інститут J.N.N., Каннігайнар, Таміл Наду 601102, Індія

⁵Національний технологічний інститут Кумо (KIT), 61 Даехак-ро, Гам-сі, Гйонгбук, 39177, Республіка Корея

^{6*}Кафедра фізики, Технологічний інститут PERI, Манніваккам, Таміл Наду - 600048, Індія, researchh.group@gmail.com

Для створення зразків CuO з двома типами морфології, таких як наночастинки (CuO-NPs) і нанострижки (CuO-NRs), використано мікрохвильове нагрівання (МНМ) та мутований золь-гель (SGM) механізми щодо рослинного екстракту *Mussaendafrondosa* як біо-оператора. Для аналізу структури, чистоти та морфологічних характеристик зразка використовували метод рентгенографії порошку (XRD), скануючу електронну мікроскопію (SEM) та енергодисперсійні X-променеві дослідження (EDX). Для аналізу оптичних властивостей та розрахунку значення енергії забороненої зони використано методології спектроскопії дифузного відбиття (DRS) і фотолюмінесценції (PL). Ширина забороненої зони зразків виміряна за допомогою механізму Кубелка-Мунка. Отримано, що вона становить 2,74 eV і 2,33 eV для CuO-NP і CuO-NR, відповідно. CuO-NP та CuO-NR досліджували на антибактеріальну активність щодо грам-позитивного та грам-негативного мікроорганізмів за допомогою модифікованого методу дискової дифузії. У співвідношенні зі зразком нанострижків CuO, антибактеріальне дослідження підтверджує, що наночастинки CuO є високоякісними антибактеріальними агентами. Використовуючи сонячне освітлення досліджено фотокаталітичну активність нанореагентів CuO (CuO-NP та CuO-NR) для розкладання барвника метилового синього (MB). Результати показали, що CuO-NP з меншими розмірами частинок розкладають MB більше, ніж CuONRs.

Ключові слова: CuO, наночастинки, *Mussaendafrondosa*; антибактеріальна активність; оптичні властивості; фотокаталітичні застосування.